

Effect of Geobags on Water Flow through Capillary Barrier System

H. Rahardjo¹, N. Gofar¹, F. Harnas², A. Satyanaga¹

¹School of Civil and Environmental Engineering, Nanyang technological University, Singapore

²Weeteveen+Bos South East Asia Pte. Ltd. Singapore

E-mail: nurlygofar@ntu.edu.sg

ABSTRACT: Capillary barrier is a two-layer cover system consisting of fine over coarse materials designed to protect slope from rainfall-induced failure. Previous studies have shown that the capillary barrier system (CBS) is effective for protection of gentle slopes, but the application of CBS on steep slopes requires further study. The fine materials are wrapped with geobags before laying them on top of the coarse materials. In this case, the bags serve as the separator between the fine and coarse materials. This paper highlights the effect of geobags on the effectiveness of CBS consisting of fine sand (Sand) as the fine material and reclaimed asphalt pavement (RAP) as the coarse material. Soil column tests were performed for two configurations (1) Sand overlying RAP (no-geo) and (2) Sand overlying RAP with geobags inserted at the interface (geo). The soil column was instrumented with tensiometer-transducer system, moisture sensors and electronic balance to measure pore-water pressures (PWP), volumetric water content (VWC) and outflow, respectively. Numerical simulations were carried out to support the findings from the soil column tests. Results of the soil column tests and numerical analyses on both configurations showed that the presence of geobags at the interface of Sand and RAP does not affect the effectiveness of CBS as slope protection from rainfall infiltration.

KEYWORDS: Geobags, Infiltration, Capillary barrier system, Soil column test, Numerical model

1. INTRODUCTION

Rainfall infiltration is a major triggering factor to slope failure in unsaturated soils because the failure mostly occurs during or after heavy rainfall (Rahardjo et al, 2000; Cho et al., 2001; Tsaparas, et al., 2002; Gofar et al, 2008). The strength of unsaturated soil is governed by two independent stress-state variables: matric suction (negative pore-water pressure, PWP) and net normal stress (Fredlund and Rahardjo, 1993). When rain-water infiltrates into unsaturated soil, the matric suction decreases, hence affecting the shear strength properties and triggers slope failure (Li et al., 2005). Previous studies (e.g. Yoo and Jung, 2006; Roy et al, 2014) showed that excessive rainfall was also the cause of many failures of reinforced soil slope. Therefore, capillary barrier system (CBS) was developed as an effective measure to minimize the loss of matric suction due to rainfall infiltration into sloping ground (Li et al., 2013 and Rahardjo et al., 2012).

The CBS is a two-layer soil cover utilizing the contrast in hydraulic properties of the fine- and coarse materials under an unsaturated condition in order to minimize water percolation (Stormont and Anderson, 1999; Khire et al., 2000; Harnas et al, 2014). The coarse material has a higher coefficient of permeability than that of the fine material in a saturated condition. However, the coefficient of permeability of coarse material decreases more significantly than that of the fine material as the negative PWP or matric suction increases. Thus, in unsaturated condition, the coefficient of permeability of coarse material is lower than the coefficient of permeability of fine material. In this condition, the coarse material acts as a barrier that limits the downward movement of water into the soil below the CBS. If water infiltrates through the fine material during a rainfall and reaches the interface of the fine-and coarse materials, it can only infiltrate the coarse material at a very slow rate. The remaining water is temporarily stored in the fine material resulting in the increase of water content. The slow rate of water flow occurs until the PWP at the interface reaches a value at which the coefficient of permeability of the coarse material is similar to the permeability of the fine material (Zornberg, et al. 2010; Khire et al. 2000). This PWP is called the breakthrough PWP and its value corresponds to the water-entry value of the coarse material. If breakthrough occurs, the coarse material is no longer acting as a barrier since the negative PWP decreases to a value below its water entry value (Stormont and Anderson, 1999). The effectiveness of a CBS depends on the water storage of the fine material and the contrast in the particle size of the fine- and coarse materials (Smersud and Selker, 2001).

The CBS has been used as protection of slopes up to about 35o inclination angle. Research works by Rahardjo et al. (2012) proved that the CBS was effective to minimize rainwater infiltration into the slope beneath CBS. As a result, the slope was maintained stable during rainfall. Construction of the CBS for protection of slope steeper than 35o requires consideration on stability aspect. Hence, the fine material was wrapped with geobags in order to protect the CBS material from sliding down (Figure 1). As the fine materials are wrapped with the bags, a significant increase in strength is achieved, therefore provide a gabion type of slope stabilization method, which has been used widely in Japan (Matsuoka and Liu, 2006) as well as other parts of the world. Geobarrier system was developed as slope protection system which combine the mechanical stabilization of steep slope through geobag wall and CBS as slope protection to minimize rainwater infiltration into the slope (Rahardjo et al, 2015).

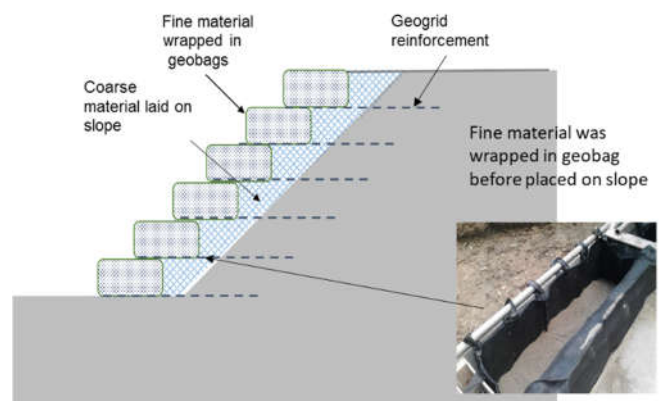


Figure 1 Capillary barrier system (CBS) on steep slope

The presence of geobag at the interface between fine and coarse materials is expected to have an insignificant effect on the effectiveness of the CBS to minimize rainfall infiltration into slope. Since there was no previous study on the effect of the geobags on the effectiveness of the CBS, this paper presents the results of a current study using soil column tests on two configurations (1) Sand overlying RAP (no-geo) and (2) Sand overlying RAP with geobags inserted at the interface (geo). The soil column was instrumented with tensiometer-transducer system, moisture sensors and electronic

balance to measure PWP, VWC and outflow, respectively. Numerical modelling of the soil column test were performed to observe the PWP and VWC distributions in the CBS system when subjected to rainfall infiltration.

2. MATERIAL PROPERTIES

Sand and RAP were used in this study as fine and coarse materials forming the CBS. The RAP was utilized in this study because waste material has been used as alternative material for construction purpose (Cardoso et al, 2016). Previous study (BCA-SIA, 2008) confirmed that the density and other physical properties of RAP are similar to natural aggregates. Grain-size distributions of Sand and RAP, determined following ASTM D422 (2007), are shown in Figure 2. The grain-size distribution indicated that both Sand and RAP can be classified as a uniformly-graded sand (SP) and uniformly graded gravel (GP) (ASTM D2487-11) with a coefficient of uniformity of 2.1 and 2.4, respectively. The ratio of d50 of RAP and d50 of Sand was 13.4, which is higher than five as an indicator of an effective CBS (Smersud and Selker, 2001). Table 1 shows the Index properties of materials used in this study.

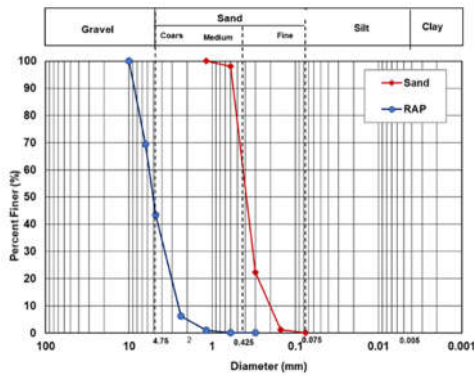


Figure 2 Grain size distribution of Sand and RAP

Table 1 Index properties of materials used in this study

Properties	Soil	
	Sand	RAP
Soil Classification (ASTM D2487-11, 2011)	Poorly Graded sand SP	Poorly Graded GP Gravel GP
Specific Gravity (ASTM D854-14, 2014)	2.65	2.48
Grain size distribution (ASTM D422-63, 2007)		
D_{60} (mm)	0.45	6
D_{30} (mm)	0.32	3.5
D_{10} (mm)	0.20	2.5
Coefficient of uniformity (C_u)	2.1	2.4
Coefficient of curvature (C_c)	1.2	0.8
Density Test (ASTM D4253-00, 2006)		
(ρ_{dmax}) (Mg/m ³)	1.69	1.70
(ρ_{dmin}) (Mg/m ³)	1.26	1.40
Dry density for Test (80% ρ_{dmax}) (Mg/m ³)	1.60	1.64

Soil Water Characteristic Curves (SWCC)s of Sand and RAP were tested in laboratory using Tempe cell. Fredlund & Xing (1994) fitting equation was used to construct the SWCC based on the laboratory data as presented in Figure 3a. The SWCC variables were calculated using equations presented in Zhai and Rahardjo (2012). Coefficients of saturated permeability of Sand and RAP were tested using constant head permeability test following ASTM D2434-68

(2006). The results indicated that the saturated coefficient of permeability of Sand (6.5×10^{-4} m/s) was two orders of magnitude lower than that of RAP (5.3×10^{-2} m/s). The permeability functions of Sand and RAP were obtained using the statistical method and best fitted using the equation proposed by Leong and Rahardjo (1997). The shape of the permeability function is similar to the shape of SWCC (Fredlund et al. 1994), thus fitting parameters (p) in the equation was selected based on the shape similarity with that of SWCC. The permeability functions of Sand and RAP are shown in Figure 3b. The p values, together with the fitting parameters from SWCC are summarized in Table 2.

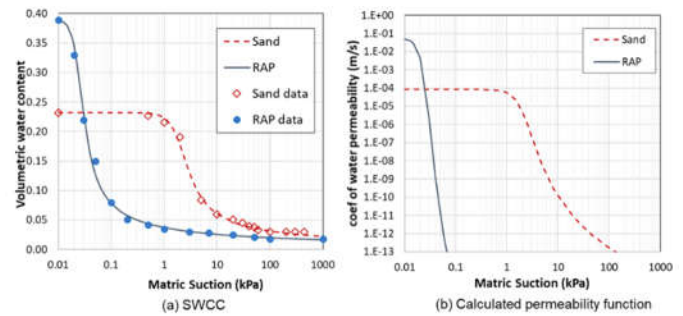


Figure 3 SWCCs and permeability functions of Sand and RAP

Table 2 SWCCs and permeability functions parameters

Parameters	Symbol	Sand	RAP
Vol. water content at saturation	θ_s	0.232	0.39
Air entry value (kPa)	ψ_a	1.20	0.015
Residual matric suction (kPa)	ψ_r	7	0.6
Residual vol. water content	ψ_r	0.042	0.05
Fredlund & Xing (1994) parameters for best fitting	a	1.796	0.023
	n	3.288	5.163
SWCC data	m	0.766	0.792
Coefficient of saturated permeability (m/s)	k_s	6.8×10^{-4}	5.3×10^{-2}
Leong's & Rahardjo (1997b) p parameter for fitting the permeability function	p	10	20

The geobags used for this study was 1 mm thick of woven geosynthetics with water coefficient of permeability of 0.2 m/s (ISO 11058). The apparent opening size of the geobags used in this study was 0.6 mm (ISO12956). In order to obtain the saturated volumetric water content (VWC) of the geobags, three specimens, of 50 mm long and 20 mm wide, were saturated by soaking them in water inside a vacuum desiccator for more than 24 h. The specimens were weighed and then dried in an oven at 105°C for about 24 h. High precision balance (accuracy of ± 0.001 g) was used for weighing the specimens. Results show that the geobags has a very low saturated VWC i.e. 0.007, and therefore very low water holding capacity.

3. SOIL COLUMN TEST

3.1 Soil Column Apparatus

Soil column experiments were performed in this study using a soil column apparatus and methods as presented in Yang et al (2004). The column was made of acrylic with a wall thickness of 5 mm. The height and the inner diameter of the acrylic column were 500 mm and 190 mm, respectively. Rainfall was applied to the surface of the column through plastic nozzles placed on top of the column. The nozzles were connected to a constant head water tank which regulates

the pressure to the nozzles. The water percolated through the soil column was drained into a constant head tank by an outlet at the base plate. The overflow from the constant head tank was directed to a container placed on an electronic weighing balance with a capacity of 12,000 g and a resolution of 1g to quantify the amount of discharge.

The soil column was equipped with tensiometer-transducer system and soil moisture sensors. The PWP was measured using small-tip tensiometer model 2100F (Soil-moisture Equipment Corporation, USA). The tensiometers consists of four main parts: high air-entry ceramic tip, tensiometer shaft, pressure transducer and jet-fill reservoir cup. The high air-entry ceramic tip had an air-entry value of 100 kPa. The pressure transducer was GT3-15 (ICT international Pty Ltd) with a pressure range of -100 to 100 kPa. The soil moisture sensor was MP306 (ICT International Pty Ltd, Australia) with three in-plane stainless steel needles. The moisture sensor adopted standing wave principle to determine the changes in VWC based on the changes in the dielectric constant of the soil. The moisture sensor can provide a measurement of VWC with an accuracy of $\pm 0.01\%$. The tensiometers, pressure transducers and the moisture sensors were calibrated prior to the test. All instruments were connected to an ICT data logger, and subsequently transmitted to a personal computer. Similarly, the weighing balance was calibrated and connected to the personal computer.

3.2. Experimental program

Two column models were investigated. The first column (no-geo) consists of 0.3 m thick Sand overlying a 0.2 m thick RAP. The second column (geo) was similar to the first column except that a geobags sheet was inserted at the interface between RAP and Sand. The schematic diagram of the column models along with the instrument locations are presented in Figure 4.

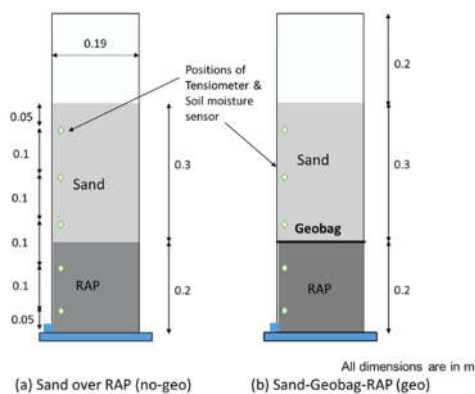


Figure 4 Soil column tests performed in this study

Prior to the placement of the material, the inner column wall was lubricated with a thin layer of vacuum grease to avoid the development of preferential water pathway during infiltration experiments. Once the soil column apparatus was set up, gravel layer was placed at the bottom of the soil column and covered with wet cloth. Careful placement of material was carried out in order to obtain a homogenous and uniform column. Firstly, dry weight of the materials for every lift was calculated. The dry density of the soils used in this study was at 80% of the maximum dry density of the materials (Table 1). The oven-dried material was placed and compacted in a 100 mm lift. Measuring instruments were installed during compaction to ensure good contact between the material and the instruments. A filter paper was placed on top of the soil column to distribute the rainfall evenly. Before the placement of the material, a thin layer of vacuum grease was applied to inside of the

column wall to avoid the development of preferential water pathway during infiltration experiments. Gravel layer was placed at the bottom of the soil column and covered with geotextile once the soil column apparatus was set up.

The PWP readings in the soil column were usually inconsistent after the compaction process. Therefore, upward flow (UF) and drawdown (DD) tests were carried out in order to obtain an appropriate initial condition before the rainfall test could be conducted. The upward flow test was aimed to saturate the soil column (removing the entrapped air) and to assess the coefficient of permeability at saturation of the material inside the column. The test was conducted until a steady-state upward flow condition was achieved. Afterwards, the valve at the bottom of the column was closed. A hydrostatic condition with the water table at the top of the column was created as the initial condition for the rapid drawdown test. The drawdown test was conducted to achieve an initial condition for the rainfall tests. The rapid drawdown test was conducted by lowering the water table from the top of the column ($z = 500$ mm) to the base of the column ($z = 0$). This initial condition was assumed as a condition following a heavy rainfall so that the capillary barrier was in a fully saturated condition and breakthrough had occurred. The rainfall test was started when equilibrium was achieved in terms of change in PWP. The water table was maintained at the bottom of the column for the rainfall test.

The soil columns were subjected to two rainfall patterns: RF1 represented high intensity long duration rainfall of 30 mm/h (equal to 8.3×10^{-6} m/s) for six hours, and RF2 represented short duration rainfall with very high intensity of 234 mm/h (equal to 6.5×10^{-5} m/s) for 1 hour. No ponding was expected since both rainfall intensities were lower than the saturated coefficient permeability of Sand (6.8×10^{-4} m/s). After conducting each rainfall test, the top of the column was closed to avoid evaporation. The experimental plan for the column study is summarized in Table 3.

Table 3 Experimental program for soil column test

Test	Rainfall Rate (m/s)	Rainfall duration (h)	Test Code	
			Column 1	Column 2
Upward saturation	–	–	no-geo;UF	geo;UF
Rapid drawdown	–	–	no-geo;DD	geo;DD
Rainfall& Drainage	8.3×10^{-6}	6	no-geo;RF1	geo;RF1
Rainfall& Drainage	6.5×10^{-5}	1	no-geo;RF2	geo;RF2

3.3 Numerical simulation of soil column test

Numerical analyses were carried out in this study using saturated/unsaturated seepage finite element code SEEP/W (GeoSlope International 2012) for the two configurations studied in the soil column tests (namely: no-geo and geo). Similar boundary conditions as the soil column tests were adopted in the numerical analysis. The rainfall was assigned at the top of the column while the bottom of the column was set at atmospheric pressure. Other boundary conditions include zero pressure ($H=0$) at the bottom of the soil column, and zero flux ($Q=0$) at the sides to control the water flow in the vertical direction only. The dimensions and finite element mesh as well as the boundary conditions adopted in the modelling of the soil column infiltration test are shown in Figure 5. The SWCCs and the permeability functions from Figure 3 were used for modelling SWCCs and permeability functions of the soils, while the geobags was modelled as saturated material with coefficient of permeability of 0.2 m/s and thickness of 1 mm.

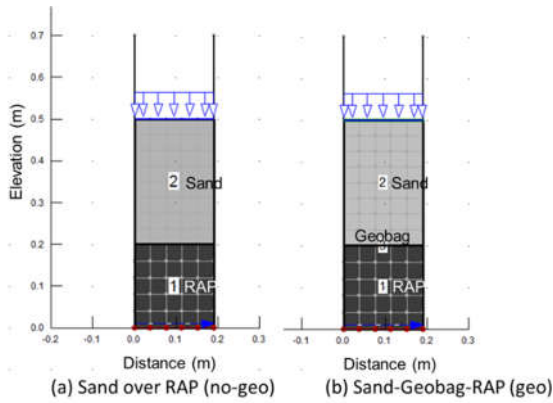


Figure 5 Finite element mesh for modelling soil column tests

4. RESULTS AND DISCUSSIONS

4.1 Initial conditions for rainfall tests

Upward saturation and drawdown tests were carried out on both configurations (no-geo and geo) to obtain the initial condition for rainfall tests. The PWP profiles after upward saturation (UF) and rapid drawdown (DD) as well as upon equilibrium after rainfall test 1 (RF1) in no-geo and geo columns are presented in Figure 6. The PWP after DD increased linearly with depth from the top of soil column to the interface between Sand and RAP, then the PWP decreased due to delay in water flow at the interface. Rainfall 1 tests (no-geo-RF1 and geo-RF1) were conducted after the PWP reached equilibrium after the DD test (about 14 days). Rainfall test 2 (no-geo-RF2 and geo-RF2) were carried out after the PWP came to equilibrium after RF1 (also about 14 days). In this case initial PWP for RF1 was the equilibrium PWP after DD test while the initial PWP for RF2 test was the equilibrium PWP after the completion of RF1 test.

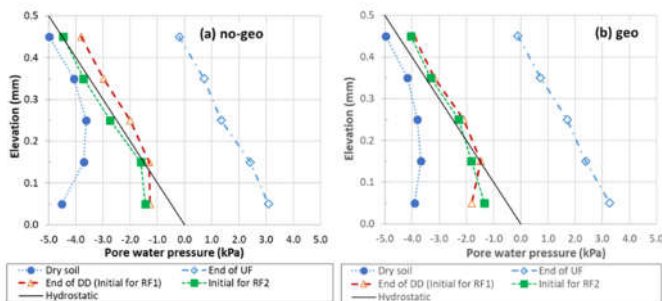


Figure 6 Initial PWP for numerical analysis of soil column test under RF1 and RF2

4.2 Rainfall tests

The PWP profiles derived from soil column tests and numerical analyses for application of RF1 (30 mm/h for 6 hours) on both no-geo and geo columns are shown in Figures. 7a and 7b. The figure indicates that, in general, the PWP in sand layer increased uniformly due to the application of RF1. The maximum PWP in no-geo column was reached one hour after the rainfall started, while for geo column, the maximum PWP was reached at 110 minutes after the rainfall started. Capillary barrier effect was observed in both no-geo and geo under the application of RF1. The water flow was hindered at the interface between Sand and RAP, before the first breakthrough occurred. After the first breakthrough, water started to drain out from the bottom of soil column, resulting in a decrease of PWP in RAP while the PWP in Sand continued to increase due to rainfall. Then the subsequent breakthroughs occurred. There were several breakthroughs occurred in both no-geo and geo columns under RF1. The PWP distribution started to redistribute and reached equilibrium after the rainfall

stopped. Both figures 7a and 7b show almost similar conditions of PWP profile. This indicated that the presence of the geobags had a minimum influence on the water flow through Sand and RAP.

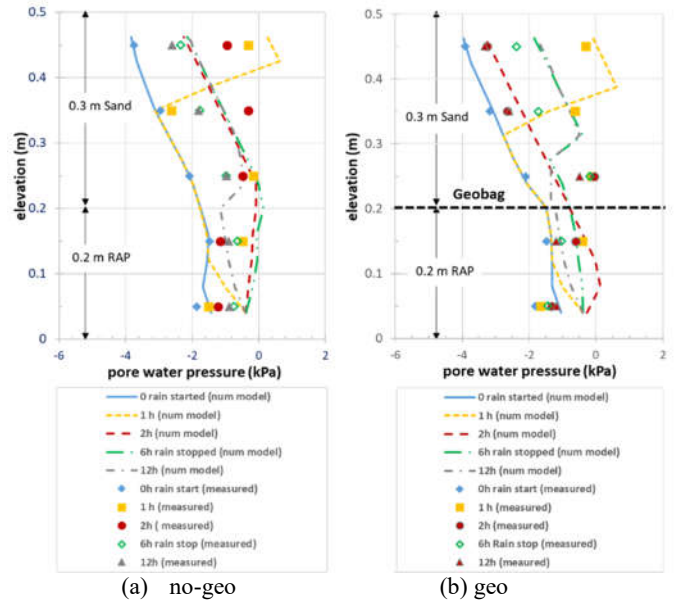


Figure 7 PWP profile in no-geo and geo columns under the application of Rainfall 1

Figures 8a and 8b show the PWP profile in no-geo and geo under the application of rainfall 2 (234mm/h for 1 h). Application of high intensity rainfall lead to significant increase in PWP at shallow depth, but the water continued to infiltrate resulting in PWP redistribution in Sand layer.

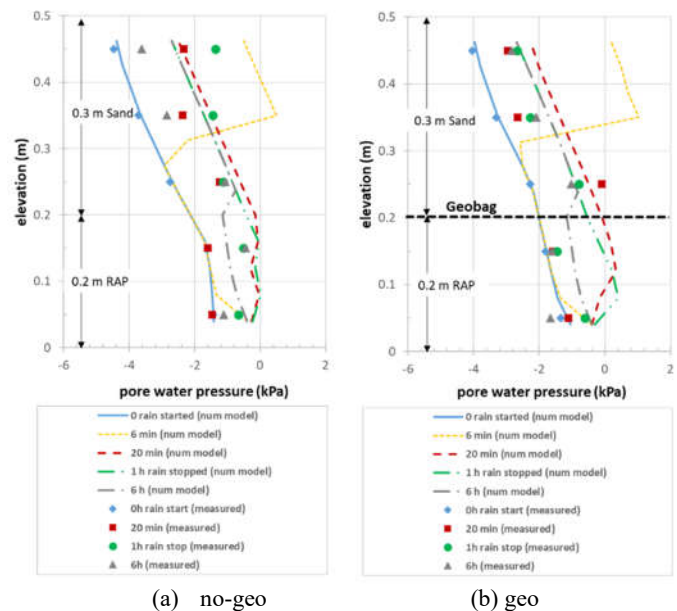


Figure 8 PWP profile in no-geo and geo under the application of RF2 (234 mm/h for 1h)

As for the application of RF1, the water infiltration was also hindered at the interface between Sand and RAP indicating that the capillary barrier was effective in both columns. Figures 8a and 8b are almost similar, even numerical analysis indicated that breakthrough occurred at the same time in no-geo and geo i.e. 16 minutes after the rainfall started. Two breakthrough were observed under RF2. The

water flow was hindered at the interface between Sand and RAP, before the first breakthrough occurred. Then the water started to drain out from the bottom of soil column, resulting in a decrease of PWP in RAP while the PWP in Sand continued to increase until the subsequent breakthrough occurred. The PWP distribution started to redistribute and reached equilibrium after the rainfall stopped. The presence of the geobags had less influence on the water flow through Sand and RAP under higher intensity rainfall.

The PWP actually fluctuated during and slightly after rainfall. Plot of the PWP above and below interface with time could give a better illustration of water flow mechanism through the interface between Sand and RAP with or without the geobags. General observation of Figure 9 indicates that the results of numerical analyses were in agreement with the results of soil column test even though measurements made during the soil column test hardly detected the fluctuation of PWP. Capillary barrier existed in both no-geo and geo columns under the application of RF1 and RF2. In addition, the transient PWP above and below interface followed the same trend in both configurations, indicating that the presence of the geobags did not change the water flow through the layered soil column. The PWP conditions after rainfall stopped were quite similar for all conditions.

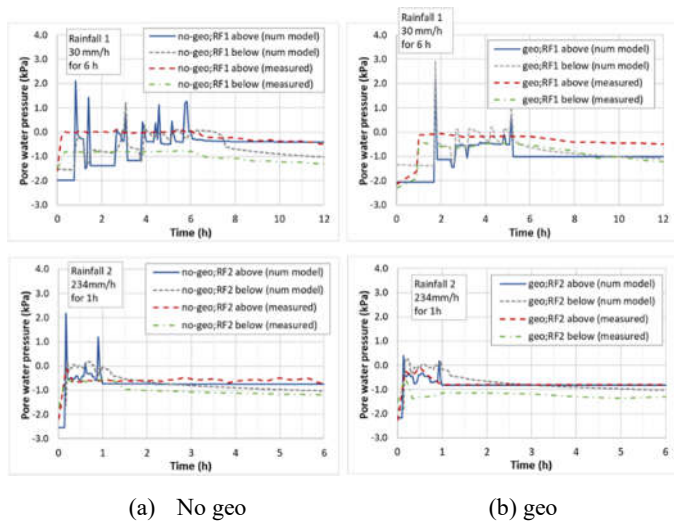


Figure 9 PWP distribution above and below interface between Sand and RAP with and without geobags interface under application of Rainfall 1 and Rainfall 2

Figure 9 shows that under the application of RF1, the PWP above and below the interface fluctuated four times during rainfall. The maximum positive PWP above the interface in no-geo was about 2.1 kPa occurred at 45 minutes after the rainfall started. In GL, the maximum PWP was 2.2 kPa that occurred 100 minutes after the rain started. The constant PWPs above interface under RF1 at equilibrium were -0.48 kPa and -1.00 kPa for no-geo and geo, respectively. The PWPs below interface under RF1 at equilibrium were -1.00 kPa for both configurations. Under the application of RF2 (234mm/h for 1h), the PWP only fluctuated twice with the maximum PWP in no-geo being 2.16 kPa occurred 105 minutes after the rainfall started. The maximum PWP above interface in geo was 0.26 kPa occurred at 16 minutes after the rainfall started. The constant PWPs above and below interface under RF2 after equilibrium were -0.73 kPa and -1.00 kPa, respectively.

The transient PWP distribution showed that despite some fluctuations at the initial stage, the PWP above and below interface converged to the same magnitude for both configurations (no-geo and geo). Observations of Figures 9 indicated that the presence of geobags had little influence on water flow mechanism through the capillary barrier system made of Sand and RAP.

Figure 10 shows the transient VWC in no-geo and geo columns above and below interface. Numerical analysis indicates that the VWC above the interface increases from the initial value to the saturated VWC of Sand i.e. 0.23, then became constant. The VWC below interface fluctuated under both rainfalls. Highest VWCs below interface were reached after each breakthrough but the VWC decreased again as the water was discharge from the bottom of the soil column. The VWC approached equilibrium when or slightly after the rain stopped. The VWC at equilibrium above interface was 0.23 i.e. the saturated VWC of Sand, while the VWC below interface was 0.03 i.e. the residual water content of RAP. General observation indicated that the VWC below interface was significantly lower than the VWC above the interface, thus the capillary barrier was effective and the presence of geobags did not influence the water flow through the Sand and RAP.

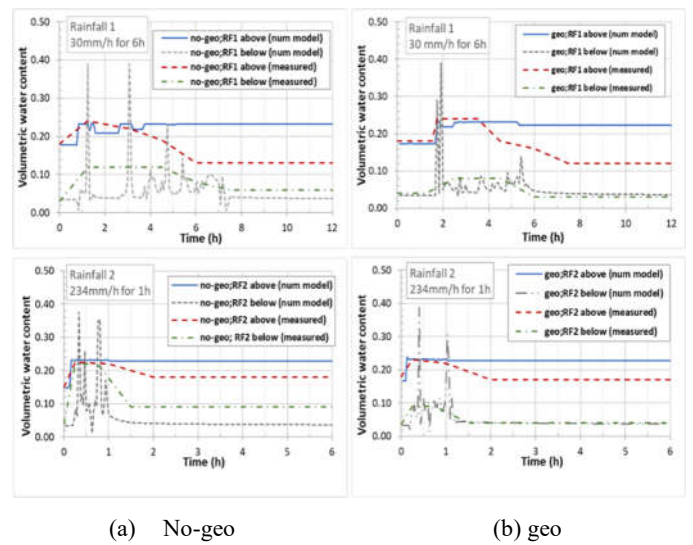


Figure 10 VWC distribution above and below interface between Sand and RAP with and without geobags interface under application of Rainfall 1 and Rainfall 2

Figure 11 shows the cumulative discharge recorded by soil column tests as compared to the results from numerical analyses. The fluctuation of discharge was observed during soil column experiment; thus accurate measurements of discharge rate was difficult.

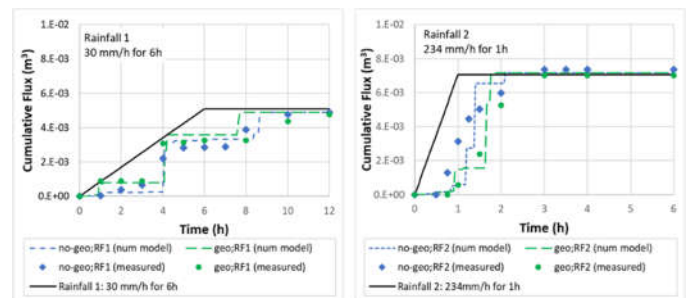


Figure 11 Cumulative discharge from soil column test and numerical model

Nonetheless, the soil column experiment indicated that there was a slightly more delay in discharge of water from no-geo configuration subjected to RF1 as compared to that of geo. Results of numerical analysis indicated discharge started in both no-geo and geo columns under RF1 after breakthrough i.e. 110 minutes after rainfall started. Significant discharge occurred about 4 hours after the rainfall started indicating second breakthrough. Other significant discharge from geo

and no-geo occurred at 7.6 hours and 8.3 hours after the rain started respectively. Under RF2, discharge started in no-geo and geo at 48 minutes after the rainfall started. The discharge continued at an increasing rate from both configurations. Discharge recorded at the bottom of the soil column supported the observation on transient PWP and VWC distribution at the interface. Capillary barrier effect can be recognized by the delay in the discharge from the bottom of soil column and the fluctuation of discharge during and slightly after rainfall stopped.

5. CONCLUSION

Geobags are required to wrap fine-grained materials to be used in CBS as a slope protection. The effect of the geobags at the interface between fine and coarse materials of CBS was evaluated in this study, based on observations of water flow through the system using soil column test and numerical analysis for two configurations: (1) Sand overlying RAP (no-geo) and (2) Sand overlying RAP with geobags inserted at the interface (geo). Results of both soil column test and numerical analysis show that capillary barrier existed in both configurations. Comparisons in the water flow mechanism in no-geo and geo in terms of PWP and VWC distribution as well as drainage from the bottom of the soil columns indicated that the presence of the geobags had an insignificant effect on the infiltration characteristics through the capillary barrier system comprising Sand and RAP. Thus, the effectiveness of CBS as protection of steep slope is not affected by the presence of geosynthetics wraparound the fine-grained material. Note that this study did not consider the possibility of clogging of geobags nor the possibility of Sand mixing with RAP.

6. REFERENCES

- ASTM (2014) D854: Standard Test Methods for Specific Gravity of Soil Solids by Water Pycnometer, ASTM International, West Conshohocken, PA. doi:10.1520/D0854-14
- ASTM (2011) D2487: Standard Practice for Classification of Soils for Engineering Purposes (Unified Soil Classification System),” Annual Book of ASTM Standards, ASTM International, West Conshohocken, PA.
- ASTM (2007) D422: Standard Test Method for Particle-Size Analysis of Soils, ASTM International, West Conshohocken, PA.
- ASTM (2006) D2434: Standard Test Method for Permeability of Granular Soil (Constant head), ASTM International, West Conshohocken, PA.
- ASTM (2006) D4253: Standard Test Methods for Maximum Index Density and Unit Weight of Soils Using a Vibratory Table, ASTM International, West Conshohocken, PA.
- ASTM (2006) D4254: Standard Test Methods for Minimum Index Density and Unit Weight of Soils and Calculation of Relative Density, ASTM International, West Conshohocken, PA.
- ASTM (2002) D6836: Standard Test Methods for Determination of the Soil Water Characteristic Curve for Desorption Using a Hanging Column, Pressure Extractor, Chilled Mirror Hygrometer, and/or Centrifuge, ASTM International, West Conshohocken, PA.
- BCA-SIA, 2008. Sustainable Architecture. Publication (2008), Issue 1. BCA Academy of Built Environment, Singapore
- Cardoso, R., Silva, R.V., de Brito, J., Dhir, R. (2016) Use of recycled aggregates from construction and demolition waste in geotechnical applications: A literature review. *Waste Management* 49:131–145
- Cho SE, Lee SR. (2001) Instability of unsaturated soil slopes due to infiltration. *Computers and Geotechnics*. 28(3):185–208.
- Fredlund, D.G., Xing, A. and Huang, S. (1994) Predicting the Permeability Function for Unsaturated Soils Using the Soil-Water Character Curve. *Canadian Geotechnical Journal*. 31(3):533-546
- Fredlund, D.G. and Xing, A., (1994) Equations for the Soil-Water Characteristic Curve. *Canadian Geotechnical Journal*. 31(3):521-532.
- Fredlund, D.G. and Rahardjo, H., (1993). *Soil Mechanics for Unsaturated Soils*. John Wiley & Sons Inc., New York, 517 pp.
- GEO-SLOPE International Ltd. (2012), *Seepage Modelling with SEEP/W*. Calgary, Alta. Canada.
- Gofar N, Lee ML, Kassim A. Response of Suction Distribution to Rainfall Infiltration in Soil Slope. *Electronic Journal of Geotechnical Engineering*. 2008;13E:13.
- Harnas, F., H. Rahardjo, E.C. Leong and J.-Y. Wang (2014). An Experimental Study on Dual Capillary Barrier using Recycled Asphalt Pavement Materials. *Canadian Geotechnical Journal*. 51(10):1165-1177.
- Khire, M. V., Benson, C. H. and Bosscher, P. J. (2000), *Capillary Barriers: Design Variables and Water Balance*. *Geotechnical and Geoenvironmental Engineering*, 126(8):695-708.
- Leong, E. C. and Rahardjo, H. (1997b). Permeability Functions for Unsaturated Soils. *Journal of Geotechnical and Geoenvironmental Engineering*. 123(12), 1118-1126.
- Li, J. H., Du, L., Chen, R. and Zhang, L. M., 2013. Numerical investigation of the performance of covers with capillary barrier effects in South China. *Computers and Geotechnics*. 48:304-315
- Li, A.G., Yue, Z.Q., Tham, L.G., Lee, C.F. and Law, K.T. (2005) Field-Monitored Variations of Soil Moisture and Matric Suction in a Saproliite Slope”. *Canadian Geotechnical Journal*, 42:13-26.
- Matsuoka, H. and Liu, S. (2006) *A new earth reinforcement method using soilbags*. London. Taylor and Francis
- Rahardjo, H., Zhai, Q., Satyanaga, A., Leong, E.C., Wang, C.L., & Wong, L.H. 2015. Geo-Barrier System as a retaining structure. In: *Proceedings of the 6th Asia-Pacific Unsaturated Soil Conference*, 24-26 Oct 2015 Guilin, PR China.
- Rahardjo, H., Santoso, V. A., Leong, E. C., Ng, Y. S. and Hua, C. J. (2012) Performance of an Instrumented Slope Covered by a Capillary Barrier System. *Journal of Geotechnical and Geoenvironmental Engineering*, 138(4):481-490.
- Rahardjo, H., Leong, E.C., Deutscher, M.S., Gasmol, J.M. and Tang, S.K. (2000) Rainfall-induced slope failures. *Geotechnical Engineering Monograph 3*, NTU-PWD Geotechnical Research Center: Singapore.
- Roy, D., Chiranjeevi K., Singh, R., and Baidya, D.K. (2009) Rainfall induced instability of mechanically stabilized earth embankments. *Geomechanics and Engineering*, 1(3): 193-204.
- Smesrud, J. and Selker, J., (2001) Effect of Soil-Particle Size Contrast on Capillary Barrier Performance. *Journal of Geotechnical and Geoenvironmental Engineering*. 127(10): 885-888.
- Stormont, J.C. and Anderson, C.E. (1999) Capillary barrier effect from underlying coarser soil layer. *Journal of Geotechnical and Geoenvironmental Engineering*, 125(8):641-648.
- Tsaparas, I., Rahardjo, H., Toll, D.G. and Leong E.C. (2002) Controlling Parameters for Rainfall-Induced Landslides. *Computer and Geotechnics*. 29:1-27.
- Yang, H., Rahardjo, H. Wibawa, B. and Leong, E.C. (2004) A Soil Column Apparatus for Laboratory Infiltration Study. *Geotechnical Testing Journal*. ASTM International. 27(4):347 – 355. Paper ID GTJ11549
- Yoo, C. and Jung, H.Y. (2006) Case history of geosynthetic reinforced segmented retaining wall failure. *Journal of Geotechnical and Geoenvironmental Engineering*. ASCE. 132(12):136-1548.
- Zhai, Q. and Rahardjo, H. (2012) Determination of Soil-Water Characteristic Curve Variables. *Computer and Geotechnics*. 42:37-43.
- Zornberg, J.G. Bouazza, A. and McCartney, J.S. (2010) Geosynthetic capillary barriers: current state of knowledge. *Geosynthetics International*. 17(5):273-300.